Mechanics Research Communications 38 (2011) 136–140

Contents lists available at ScienceDirect

Mechanics Research Communications

journal homepage: www.elsevier.com/locate/mechrescom

Virtual improvement of ice cream properties by computational homogenization of microstructures

Toufik Kanit[a,*], Samuel Forest[b], Dominique Jeulin[b,c], Franck N'Guyen[b], Scott Singleton[d]

[a] Laboratoire de Mécanique de Lille, CNRS UMR 8107, 59655 Villeneuve d'Ascq, France
[b] MINES ParisTech, Centre des Matériaux, CNRS UMR 7633, BP 87, 91003 Evry Cedex, France
[c] MINES ParisTech, Centre de Morphologie Mathématiques, 35, rue Saint-Honoré, 77305 Fontainebleau, France
[d] Unilever Colworth Research Laboratory, UK

ARTICLE INFO

Article history:
Received 29 March 2010
Received in revised form 4 November 2010
Accepted 7 January 2011
Available online 14 January 2011

Keywords:
Homogenization
Design of virtual microstructures
RVE
Elastic and thermal properties

ABSTRACT

Optimal shape design of microstructured materials has recently attracted a great deal of attention in materials science. The shape and the topology of the microstructure have a significant impact on the macroscopic properties. This paper presents different computational models of random microstructures, to virtually improve the physical properties of ice cream. Several sensory properties of this heterogeneous material issued from food industry are directly controlled by the elastic and thermal conducting ones. The material effective elastic and thermal conducting properties are obtained through direct large scale numerical simulations. The different formulations address the problem of finding the shape of the representative microstructural element for random heterogeneous media that increase the elastic moduli and thermal conductivity compared to existing products. The computational models are established using finite element method and images of virtual microstructures. In this paper we propose a new model of microstructures. This model is constructed with hexagonal prismatic rods and plates with volume fractions around 0.7 for the hard phase represented by hexagons of ice. A comparison between three two-phase elastic heterogeneous microstructures models is drawn. This illustrates the concept of design of microstructures using computational homogenization tools.

1. Introduction

Traditionally, materials are selected from a materials database of physical properties. However, the paradigm is now evolving into designing materials concurrently with morphologies to meet specific performance requirements. Material by design is a new methodology well known for structural application, see Gilormini and Bréchet (1998), Wegst and Ashby (2002), Cousin and Ashby (2003), Sirisalee et al. (2006) and Bouaziz et al. (2008).

The present work considers the study of the morphology of random linear elastic and linear thermally conducting two-phase microstructures of ice cream in order to obtain a wanted physical properties (elastic moduli and thermal conductivity). It shows that the computational homogenization makes it possible to construct new morphologies that are not investigated experimentally. The characterization of the effective material properties in this setting is made through the use of the numerical homogenization based on a representative volume element (RVE). Homogenization methods are used to predict the effective properties of these composite materials and to optimize the morphology of the microstructure. The aim of this study is to estimate the effective properties of new simulated microstructures and to compare them with real microstructures of ice cream.

2. Materials and methods

Three different morphologies are studied, 3D real images of ice cream obtained by confocal microscopy and two models of virtual composites: 3D Boolean models of prismatic hexagonal rods and plates and the Vorono mosaics, as examples of microstructures that we expect to be stiffer and more thermally conducting than the real samples of ice cream.

All the microstructures are considered as a two-phase linear elastic and linear thermally conducting materials. The elastic properties (Young's modulus E, Poisson coefficient ν, bulk modulus k) and the thermal conductivity λ are: [E (MPa), ν, k (MPa), μ (MPa), λ (Wm^{-1} K^{-1})] = [2500, 0.3, 2083, 962, 2.44] for ice with volume fraction $P_1 = 0.7$ and [25, 0.49, 417, 8, 0.0244] for cream with volume fraction $P_2 = 0.3$.

* Corresponding author. Tel.: +33 3 20 43 42 43; fax: +33 3 20 33 70 88.
E-mail address: toufik.kanit@univ-lille1.fr (T. Kanit).

0093-6413/$ – see front matter © 2011 Elsevier Ltd. All rights reserved.
doi:10.1016/j.mechrescom.2011.01.005

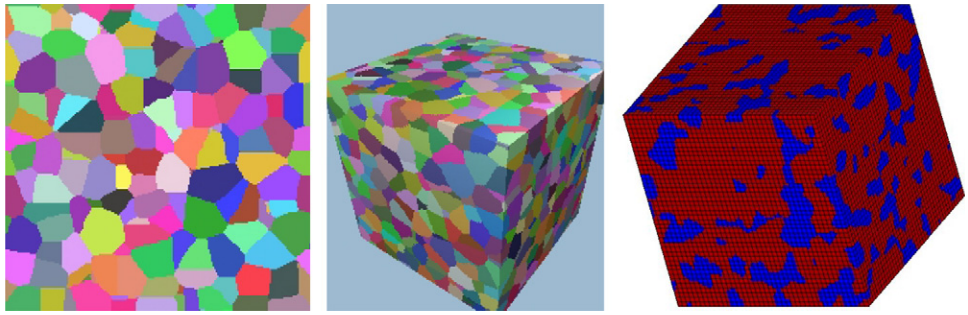

Fig. 1. Voronoï mosaics: images in 2D, 3D and finite element mesh of two-phase microstructure.

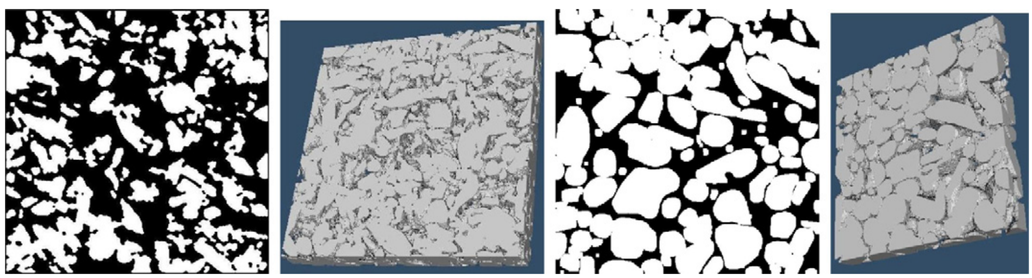

Fig. 2. Real microstructures, sample SA (left) and sample SB (right): images in 2D and 3D.

2.1. *Voronoï mosaics*

The Voronoï mosaics is a good candidate to generate virtual random media. To generate such microstructures, an original method was proposed with numerous extensions of the classical model (Decker and Jeulin, 2000), see Fig. 1.

2.2. *Three-dimensional real microstructures of ice cream*

Experimental batches of our ice cream composite were produced in blocks which are stored at −18 °C, see Kanit et al. (2006). They are used for confocal imaging. Two different types of microstructures are studied here. The first one with additive named *SA*, the second without additive named *SB*, see Fig. 2. The additive only changes the morphology of the phases but does not affect the properties of the individual phases. The samples *SB* contain fairly round ice crystals while the samples *SA* have more elongated hard phase crystals.

The mechanical test used for the determination of the effective mechanical properties is a four-point bend test, see Fig. 3. The samples used in those tests are 250 μm × 250 μm × 30 μm bars, which placed between two pairs of steel rolls used as load applicators. The two upper rolls are immobile while the two lower ones are able to apply a vertical displacement on the sample. The different values of the load *F* and the displacement of the lower rolls δ are the output of this test. The bending tests were performed over a large range of the volume fractions of phase P_1. The results are reported in Fig. 3. Note that for all volume fractions, *SA* is found to be significantly stiffer than *SB*. This difference can be explained by the role of morphology of phases in each material. The samples with additive *SA* give a higher value of Young's modulus by comparison with samples without additive *SB* for the same value of volume fraction, which can be explained by the role of more elongated hard phase crystals in samples with additive.

2.3. *Boolean models with hexagonal prismatic grains*

A good generic model to reproduce the morphology of the ice cream microstructure is the Boolean model (Matheron, 1967). The Boolean model is generated in two steps: random germs are given by points of a *Poisson point process* with intensity ρ points per unit volume. In a second step, random grains are located on the random germs, with permitted overlaps of the grains. It is known that for this model the percolation threshold is lower for anisotropic grains, such as cylindrical fibres (Jeulin and Moreaud, 2006). In the studied microstructures here, we propose to use hexagonal prismatic

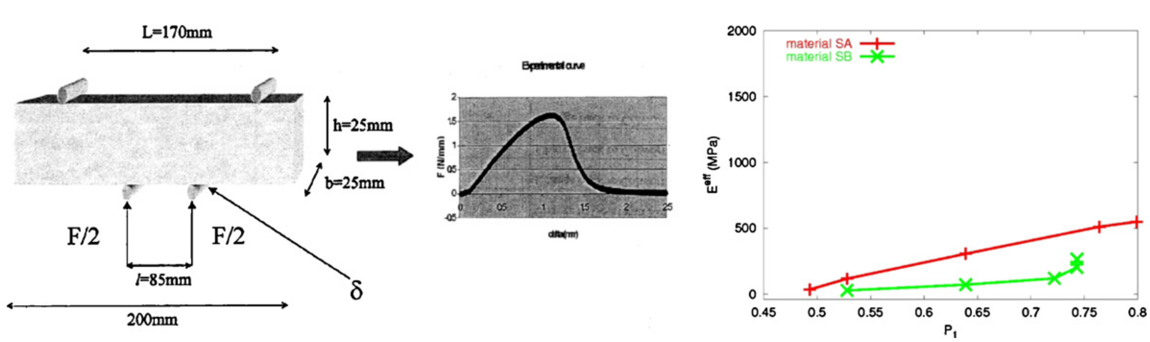

Fig. 3. The four-point bend test used to estimate the Young modulus and the experimental results.

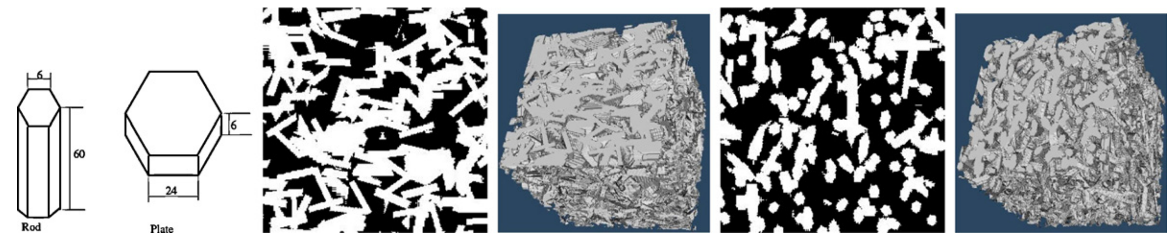

Fig. 4. Geometry and dimensions of the used primary grains in hexagonal microstructures and Boolean model (*P*50 at left and *R*50 at right): images in 2D and 3D.

primary grain for the ice phase, in order to reproduce the well-known morphology of ice crystals. The geometry and the dimensions of the used prismatic hexagons are shown in Fig. 4. Two different types of geometry were studied: one is based on hexagonal plates (microstructures named *P*50 and *P*70) and the second one is based on hexagonal rods (*R*50 and *R*70). Two volume fractions P_1 of the hard phase, represented by hexagonal prisms, were generated: 0.5 (*P*50 and *R*50) and 0.7 (*P*70 and *R*70).

3. Results

The same methodology as for the direct computations of the apparent properties for the real microstructures (Kanit et al., 2006), and for the Vorono mosaics (Kanit et al., 2003), is used here to find the apparent elastic moduli for the Boolean models with hexagonal prismatic grains. Values of the elastic properties of the two phases used for the real microstructures are also the same used in this case. The different apparent coefficients of the elasticity matrix are computed with kinematic uniform boundary conditions (KUBC), see Kanit et al. (2003) for more details about this type of boundary conditions. To study the mechanical anisotropy of our materials, we compute and provide the apparent elasticity moduli matrices. The matrices can be anisotropic if the size of the samples is not large enough to represent a deterministic size of RVE. The apparent elastic matrix C^{app} is related to the macroscopic strain tensor E and the average microscopic stress tensor $\langle\sigma\rangle$ by:

$$\langle\sigma\rangle = C^{\text{app}} : E$$

To compute the apparent elastic coefficients C_{ij}^{app}, we impose a loading strain tensor E and with the volume average local stress tensor $\langle\sigma\rangle$ we compute the coefficients C_{ij}^{app}. The apparent elastic coefficients are given by the following matrices:

$$SA = \begin{pmatrix} 1152 & 352 & 415 & 0 & 0 & 6 \\ & 1098 & 401 & 7 & 5 & 1 \\ & & 1597 & 1 & 9 & 12 \\ & & & 377 & 3 & 2 \\ & & & & 444 & 1 \\ & & & & & 451 \end{pmatrix}$$

$$SB = \begin{pmatrix} 1197 & 333 & 416 & 1 & 12 & 23 \\ & 1060 & 384 & 5 & 20 & 7 \\ & & 1675 & 1 & 37 & 34 \\ & & & 387 & 12 & 0 \\ & & & & 457 & 1 \\ & & & & & 489 \end{pmatrix}$$

$$R50 = \begin{pmatrix} 886 & 284 & 283 & 6 & 2 & 4 \\ & 783 & 273 & 5 & 3 & 1 \\ & & 654 & 0 & 4 & 1 \\ & & & 260 & 3 & 2 \\ & & & & 240 & 3 \\ & & & & & 259 \end{pmatrix}$$

$$R70 = \begin{pmatrix} 1520 & 574 & 574 & 3 & 2 & 1 \\ & 1670 & 601 & 5 & 3 & 7 \\ & & 1653 & 3 & 4 & 3 \\ & & & 492 & 8 & 2 \\ & & & & 514 & 2 \\ & & & & & 492 \end{pmatrix}$$

$$P50 = \begin{pmatrix} 527 & 200 & 199 & 5 & 2 & 2 \\ & 668 & 220 & 5 & 1 & 6 \\ & & 653 & 7 & 2 & 3 \\ & & & 185 & 5 & 2 \\ & & & & 208 & 2 \\ & & & & & 181 \end{pmatrix}$$

$$P70 = \begin{pmatrix} 1487 & 494 & 493 & 4 & 2 & 1 \\ & 1339 & 476 & 2 & 5 & 1 \\ & & 1357 & 1 & 8 & 1 \\ & & & 447 & 1 & 3 \\ & & & & 422 & 1 \\ & & & & & 447 \end{pmatrix}$$

One can notice some anisotropy of the obtained apparent elastic matrices computed for each sample. The values of the apparent elastic coefficients of the ice cream microstructures are in general not very different in the two large directions of the 3D confocal image. In the thickness direction it is not the case. As a result, the real samples of ice cream exhibit a significant anisotropy in the thickness direction. Physically, the elastic modulus value along the thickness of the sample is smaller than along the two other directions. The small thickness of the samples is responsible for this anisotropy. To quantify the anisotropy of these apparent elastic matrices, we give here the anisotropic index a for each microstructure. In the case of a matrix with a cubic symmetry, this index is given by: $a = 2C_{44}/(C_{11} - C_{12})$. In our case, we take: $C_{44} = (C_{44}^{\text{app}} + C_{55}^{\text{app}} + C_{66}^{\text{app}})/3$, $C_{11} = (C_{11}^{\text{app}} + C_{22}^{\text{app}} + C_{33}^{\text{app}})/3$ and $C_{12} = (C_{12}^{\text{app}} + C_{23}^{\text{app}} + C_{31}^{\text{app}})/3$. We can also look at the anisotropy in the plane (XY) for the real microstructures, for example. The in-plane anisotropy index a_{XY} is defined as: $a_{XY} = 2C_{44}^{\text{app}}/(C_{11}^{XY} - C_{12}^{\text{app}})$, with: $C_{11}^{XY} = (C_{11}^{\text{app}} + C_{22}^{\text{app}})/2$. The values of the retained anisotropy index for each microstructure are given in Table 1. The apparent matrices of elasticity found are quasi isotropic. The results of Table 1 suggest that the size of our microstructures is representative, as far as the isotropy is concerned. In Table 1, a comparison of values of the effective prop-

Table 1
Results of numerical simulations and index of elastic anisotropy. Notations: (S): numerical simulations, (E): experimental results, VM: Vorono mosaics. An index close to 1 corresponds to an isotropic elastic behaviour.

Microstructure	*R50*	*R70*	*P50*	*P70*	*SA*	*SB*	VM
a	1.02	0.97	0.93	0.97	0.95	0.95	
a_{XY}					0.975	0.973	
μ^{eff} (MPa) (S)	253	449	191	439	345	207	433
k^{eff} (MPa) (S)	449	916	333	781	634	334	1198
E^{eff} (MPa) (S)	639	1158	481	1109	876	515	1159
E^{epp} (MPa) (E)					384	151	
λ^{eff} (W/mK) (S)					1.2	0.77	1.346

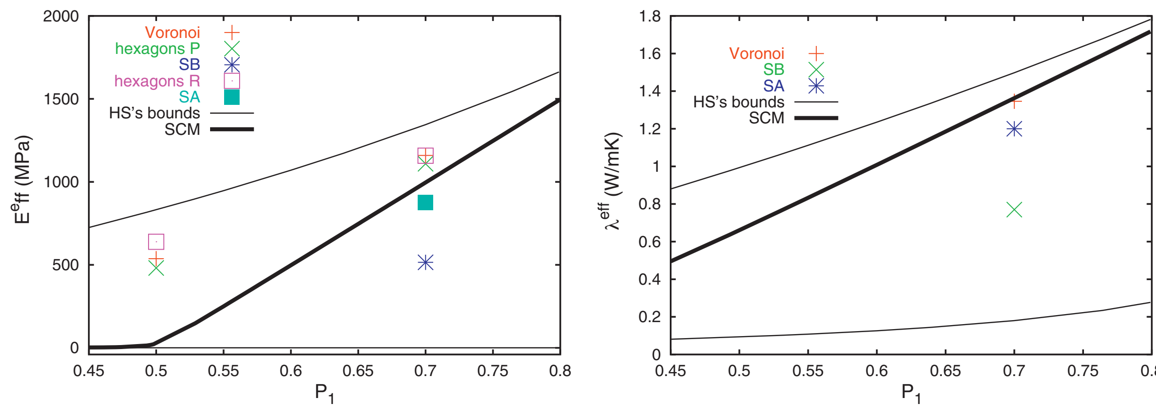

Fig. 5. Comparison of effective Young's modulus and effective thermal conductivity of three types of random two-phase elastic and linear thermal conducting materials, as a function of ice volume fraction P_1.

erties is given. Microstructures with hexagonal rods are stiffer than those with hexagonal plates. It can be explained by the fact that the hard phase in the microstructure with rod hexagons is more connected than in the other case, because of the anisotropic geometry of primary grains. The effect is more pronounced for microstructures with $P_1 = 0.5$. One can remark also that the effective Young's modulus E^{eff} of ice cream, obtained by homogenization method, is greater than the experimental one E^{app}, which can be explained by the fact that the size of the used specimens is not large enough by comparison with the RVE size.

4. Discussion and conclusion

A general conclusion concerning the physical properties can be drawn from the comparison between three types of random two-phase materials. The comparison is limited to the effective Young's modulus and the effective thermal conductivity, but can be generalized to other physical properties, see Table 1. The only difference between the three types of microstructures is the morphology of phases. Results of the comparison are given in Fig. 5. In this figure, a comparison of the effective Young's moduli of different microstructures is given by one hand and a comparison between the effective Young's modulus and the apparent (experimental) one of ice cream by the other hand. Fig. 5 gives also a comparison of the effective thermal conductivity of ice cream and Vorono mosaics. Because of the strong contrast in properties of phases, the Hashin–Shtrikman's (HS) upper and lower bounds are very far apart. The self consistent estimate (SCM), based on a spherical geometry, cannot properly take into account the effect of the morphology on the effective properties, since it is well known that when this model is applied to a porous medium, the effective Young's modulus vanishes. For the considered virtual microstructures models, the self consistent model underestimates the effective elastic properties, but gives a good estimation of the effective thermal conductivity. For the real microstructures, it overestimates these effective properties. This difference between the estimation of the self consistent model and numerical simulations results becomes more important for volume fractions P_1 close to 0.5. One finds no direct relation between the relevance of the self consistent estimate and a specific morphology. The two virtual microstructures give higher effective properties than those given by the real microstructures. It is due to the more elongated shape of grains of the existing hard phase in the virtual models, as compared to the real microstructures. The Vorono mosaics and the hexagonal microstructures give similar effective properties. A higher stiffness for the hexagonal microstructures with rod-like hard phase is found for volume fractions around 0.5.

The present work can be considered as a first step towards a computational approach of the design of microstructures. As shown in this study, in the case of products from food industry, the computation homogenization approach makes it possible to explore new morphologies that are currently not investigated experimentally, and possibly discover new products with improved properties.

As conclusion of this work, and for the sake of brevity, two important conclusions are noted:

- the effective elastic moduli and the effective thermal conductivity given by virtual models are higher than those given by the real materials.
- The Boolean microstructures with rod hexagons are stiffer than with plate hexagons.

Finally, one notes that corresponding process conditions to obtain real microstructures close to these Boolean models must be found for practical applications.

References

Bouaziz, O., Bréchet, Y., Embury, J., 2008. Heterogeneous and architectured materials: a possible strategy for design of structural materials. Advanced Engineering Materials 10, 24–36.
Cousin, J.P., Ashby, M., 2003. Materials and design, the art and science of material selection in product design. Architecture d'aujourd'hui 347, 130.

Decker, L., Jeulin, D., 2000. Simulation 3D de matériaux aléatoires poly-cristallins. La Revue de Metallurgie – CIT/Science et Génie des Matériaux Février 2000, 271–275.
Gilormini, P., Bréchet, Y., 1998. Syntheses: mechanical properties of heterogeneous media: which material for which model? Which model for which material? Modelling and Simulation in Materials Science and Engineering 7, 805–816.
Jeulin, D., Moreaud, M., 2006. Percolation of multi-scale fiber aggregates. In: Lechnerova, R., Saxl, I., Benes, V. (Eds.), S4G, 6th Int. Conf. Stereology, Spatial Statistics and Stochastic Geometry, Prague, 26–29 June 2006, Union Czech Mathematicians and Physicists, pp. 269–274.
Kanit, T., Forest, S., Galliet, I., Mounoury, V., Jeulin, D., 2003. Determination of the size of the representative volume element for random composites: statistical and numerical approach. International Journal of Solids and Structures 40, 3647–3679.
Kanit, T., Nguyen, F., Forest, S., Jeulin, D., Reed, M., Singleton, S., 2006. Apparent and effective physical properties of heterogeneous materials: representativity of samples of two materials from food industry. Computer Methods in Applied Mechanics and Engineering 195, 3960–3982.
Matheron, G., 1967. Elements pour une theorie des milieux poreux. Masson, Paris.
Sirisalee, P., Ashby, M.F., Parks, G.T., Clarkson, P.J., 2006. Multi-criteria material selection of monolithic and multi-materials in engineering design. Advanced Engineering Materials 8, 48–56.
Wegst, U.G.K., Ashby, M.F., 2002. Materials selection and design of products with low environment impact. Advanced Engineering Materials 4, 378–383.